

Direct fifth-order electronically nonresonant Raman scattering from CS₂ at room temperature

David A. Blank, Laura J. Kaufman, and Graham R. Fleming^{a)}

Department of Chemistry, University of California, and Physical Biosciences Division, Ernest Orlando Lawrence Berkeley National Laboratory, Berkeley, California, 94720

(Received 1 February 2000; accepted 4 April 2000)

In this paper we report the measurement of the direct fifth-order electronically nonresonant intermolecular response from liquid CS₂ at room temperature. We recently demonstrated that all previous attempts to measure the direct fifth-order response were dominated by third-order cascaded signals [J. Chem Phys. **111**, 3105 (1999)]. Here we show that phase matching considerations can be used to provide substantial discrimination against the cascaded third-order signals, and the direct fifth-order response can be measured. The measured responses indicate that the intermolecular spectrum of liquid CS₂ at room temperature is well described as homogenous. Comparisons of the data to simulations are discussed. © 2000 American Institute of Physics. [S0021-9606(00)00625-5]

I. INTRODUCTION

The extension of time-domain nonresonant Raman spectroscopy to fifth-order with two adjustable time delays was originally proposed by Tanimura and Mukamel as a means to separate the homogeneous and inhomogeneous contributions to vibrational line shapes.¹ Following its inception, the technique received considerable attention both theoretically and experimentally.^{2–26} The experiment involves an initial Raman excitation of the system by two ultrafast laser pulses leading to a superposition state. After the first time delay a second set of pulses coherently transfers the system to a second superposition state, and following the second time delay a final pulse interrogates the system via a stimulated Raman scattering event. This sequence of events is shown schematically with a ladder diagram in Fig. 1. The ability to separate the homogeneous and inhomogeneous contributions to line shapes comes from the potential for the two superposition states to appear as complex conjugates with nearly equal and opposite time evolution frequencies.¹ The result is a rephasing event analogous to that found in electronic echo spectroscopy, which can remove the inhomogeneous contribution to the electronic line shape.²⁷

Shortly after the initial proposal, it was realized that, beyond the ability to separate homogeneous and inhomogeneous contributions to the line shape, the technique also had the potential to probe the coupling between nuclear motions. Generation of the fifth-order nonresonant Raman signal requires either nonlinearity in the field-matter interaction or anharmonicity in the mechanical potential.^{3,23} It is this requirement that provides the potential for the technique to reveal the couplings between the basis modes that describe the nuclear motions. The inherent dependence of the signal on either the nonlinearity in the polarizability or the anharmonicity in the mechanical potential means that the technique is an exquisitely sensitive probe of one or both of these nonlinearities. This is compared with the lower- (third-) or-

der nonresonant Raman signals that are typically dominated by responses that are linear in the polarizability and lacking in sensitivity to the mechanical anharmonicity. The requirements for the generation of the direct fifth-order signal also mean that the signal intensities will be significantly diminished compared with signals that have no such requirements. As a result, signals from cascading lower-order processes can become competitive with, or even substantially larger than, the desired signal from the direct process.

We have recently demonstrated experimentally that the previously measured fifth-order nonresonant Raman signals from CS₂ are dominated by cascading third-order signals.²⁶ In this manuscript we show that by using an appropriately chosen phase matching geometry it is possible to provide substantial discrimination against the cascaded signals and measure the direct fifth-order Raman signals generated by the intermolecular motions in CS₂.

II. EXPERIMENT

A. Experimental setup

A regeneratively amplified Titanium Sapphire laser system provided 25 μ J/pulse, 42 (fs) femtosecond (Gaussian, full width at half of maximum intensity), 800 nm pulses at a repetition rate 1.5 kHz.²⁸ The pulse duration was determined by off-axis autocorrelations in a 150 μ m BBO crystal. The regenerative amplifier was pumped by a Q-switched, diode-pumped Nd:YAG (LightWave Electronics) with shot-to-shot root-mean-squared intensity fluctuations at 532 nm of <0.5% leading to very small power fluctuations at our sample. Following attenuation of the power, the pulse was split into five pulses of nearly equal intensity, 2–4 μ J per pulse per beam. The five beams were timed mechanically and the relative polarization of each beam was individually adjusted using a $\lambda/2$ wave plate. The two adjustable time variables were swept using mechanical translation stages with stepping resolution of 0.1 μ m (Newport). The five beams were focused into a 1.0 mm sample cell containing CS₂ at room temperature using a 28.9 cm focal length singlet

^{a)}Electronic mail: grfleming@lbl.gov

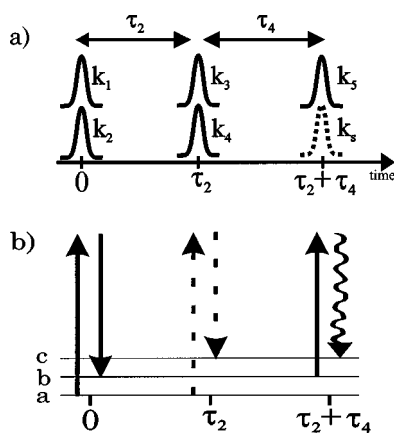


FIG. 1. (a) Diagram showing the pulse sequence and the labels for the adjustable time variables for the fifth-order experiment. (b) Ladder diagram showing one of the Liouville pathways. The solid lines represent a ket side interaction and the dashed lines represent a bra side interaction. The wavy line is the stimulated emission of the signal.

lens. The fifth-order signal was generated in a unique direction, as discussed in the phase matching section below. An iris was used to spatially select the signal, which was then detected using an IR extended photomultiplier tube (Hamamatsu, R636-10). The very low intensity of the signal required that a tracer pulse be sent along the signal direction for the purpose of aligning the spatial selection of the signal. One of the five incoming beams was mechanically chopped at half the laser repetition rate, and the signal was collected using lock-in amplification at the chopping frequency.

B. Phase matching considerations

We have previously demonstrated that, for the intermolecular motions in liquid CS_2 , cascading third-order responses are much larger in magnitude than the direct fifth-order response.²⁶ In this manuscript we demonstrate how phase matching considerations can be used to discriminate against the cascaded responses, and since phase matching will provide the key to detection of the direct fifth-order signal we will discuss this issue in some detail. Both the direct and cascaded scattering processes generate a signal along the same phase matched direction. However, it is possible to decrease the magnitude of the cascaded signals by arranging the five incoming beams in a geometry that provides a significant phase mismatch for the first step of each cascaded process.

We measure the signal along the phase matched direction $k_{s5} = k_1 - k_2 - k_3 + k_4 + k_5$. As previously discussed in detail, there are four possible third-order cascade processes that can generate a signal along this same phase matched direction.^{25,26,29} Two of the cascaded signals result in time-dependent responses that are symmetric in the two adjustable time variables. We will refer to these cascades as sequential, with their first steps defined by the wave vectors $k_{s1} = k_1 - k_2 - k_3$ and $k_{s2} = k_1 - k_2 + k_4$. The field emitted by the first step, a third-order scattering event, serves as one of the two fields involved as the pump step in a third-order process on a different chromophore. In the other two cascade processes the field emitted in the first step participates as a probe field

TABLE I. Beam angles. These are the angles of the incoming beams *within the liquid CS_2 sample* for the geometry shown in Fig. 2. Theta is the azimuthal angle measured counterclockwise from the positive x axis and phi is the elevation from the z (propagation) axis. All angles are in degrees.

Beam	Theta	Phi
1	-22.0	1.8
2	-154.6	1.6
3	-133.7	0.9
4	-40.3	0.1
5	158.2	2.4

in a second third-order scattering event on a separate chromophore. The first step for these two cascades are defined by the wave vectors $k_{p1} = k_1 - k_2 + k_5$ and $k_{p2} = -k_3 + k_4 + k_5$, and we will refer to these cascades as parallel. The time-dependent responses for both types of cascades, in terms of the third-order response functions, are shown in Eqs. (1a) and (1b):

$$R_{nmlkji, \text{sequential}}^{(3)^2} = R_{\text{seq}}^{(5)}(\tau_2, \tau_4) = R_{\sigma k ji}^{(3)}(\tau_2) R_{nml \sigma}^{(3)}(\tau_4) + R_{\sigma k ji}^{(3)}(\tau_4) R_{nml \sigma}^{(3)}(\tau_2), \quad (1a)$$

$$R_{nmlkji, \text{parallel}}^{(3)^2} = R_{\text{par}}^{(5)}(\tau_2, \tau_4) = R_{\sigma m ji}^{(3)}(\tau_2 + \tau_4) R_{n \sigma lk}^{(3)}(\tau_4) + R_{\sigma ml k}^{(3)}(\tau_4) R_{n \sigma ji}^{(3)}(\tau_2 + \tau_4). \quad (1b)$$

The subscripts, $i-n$, refer to the relative polarizations of the incoming laser fields and the signal field. By convention the time ordering of the interactions labeled by the subscripts reads from right to left beginning with the first interaction pulse and ending with the emitted signal.

The phase matching factor is typically expressed as $\text{sinc}(\Delta k l / 2)$, where Δk is the difference between the incoming wave vectors and the signal wave vector and l is the path length through the sample.³⁰ One of the assumptions required to obtain the $\text{sinc}(\Delta k l / 2)$ term in the final expression is that the incoming beams are propagating colinearly, i.e., there is no variation in the product of the amplitudes of the incoming beams as a function of the distance along the sample, z . Although our incoming beams do approach the sample at small angles from the normal of the sample face, see Table I, there is still a significant z dependence of the amplitude product of the incoming beams within our 1 mm sample pathlength, as illustrated in Fig. 2. In our previous paper we made a limited attempt to account for the physical crossing of the incoming beams by using the calculated amplitude product to determine an effective pathlength that was subsequently used as l in the $\text{sinc}(\Delta k l / 2)$ phase matching term.²⁶ Here we account for the physical crossing of the incoming beams, as it pertains to the degree of phase matching, in a more detailed manner.

We start from the Maxwell equation for the amplitude of the signal field using the n -order induced polarization as the source term,

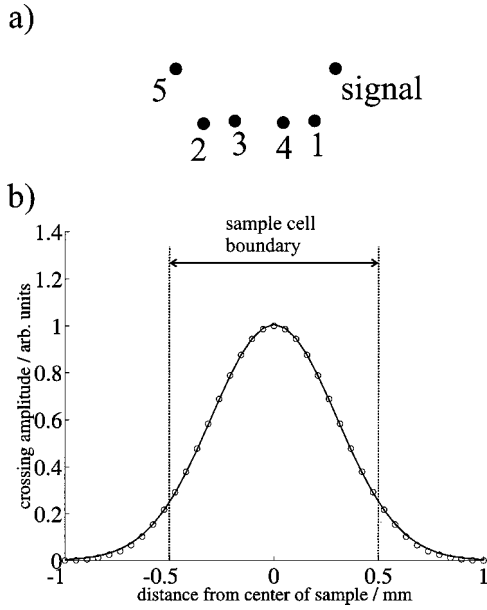


FIG. 2. (a) Diagram showing the relative positions of the five incoming beams and the signal in the x - y plane orthogonal to the propagation axis, z . (b) The open circles are the calculated amplitude product for the five incoming beams as a function of the propagation axis, z . The solid line is a fit to the calculated distribution using a Gaussian distribution with a FWHM = 0.71 mm.

$$\nabla \times \nabla \times [\varepsilon_s^{(n)}(r, t) \exp(ik_{s2} \cdot r)] - \frac{n_s^2 \omega_s^2}{c^2} \varepsilon_s^{(n)}(r, t) \exp(ik_{s2} \cdot r) = \frac{4\pi\omega_s^2}{c^2} \bar{P}_s^{(n)}(t) \times \exp(ik_{s1} \cdot r), \quad (2)$$

where \mathbf{k}_{s1} is the combination of incoming wave vectors and \mathbf{k}_{s2} is the wave vector of the generated field. One finds a solution of the form³⁰

$$\varepsilon_s^{(n)}(t) = 2\pi i \frac{\omega_s^2}{k_{s2} c^2} \int dz P_s^{(n)}(t, z) \exp(i \Delta k \cdot z), \quad (3)$$

with $\Delta k = k_{s1} - k_{s2}$. The n -order induced polarization can be expressed in terms of the n -order response function, $R^{(n)}$,

$$P^{(n)}(t_1, \dots, t_{(n/2-1)}, z) = NA^{(n)}(z) R^{(n)}(t_1, \dots, t_{(n/2-1)}), \quad (4)$$

where $A^{(n)}(z)$ refers to the z -dependent amplitude product of the n incoming fields, $\varepsilon_1(z)\varepsilon_2(z)\dots\varepsilon_n(z)$, and N is the number density.

Expressing $A^{(n)}(z)$ as the normalized spatial z -dependent overlap of the n incoming beams, $a^{(n)}(z)$, times the magnitude of the product of the n incoming beams when perfectly overlapped, $A^{(n)}$, the signal field amplitude becomes

$$\varepsilon_s^{(n)}(t_1, \dots, t_{(n/2-1)}) = 2\pi i \frac{\omega_s^2}{k_{s2} c^2} NA^{(n)} \times R^{(n)}(t_1, \dots, t_{(n/2-1)}) \int_0^l dz \times a^{(n)}(z) \exp(i \Delta k \cdot z). \quad (5)$$

TABLE II. Phase matching factors. These are the phase matching factors, calculated from Eq. (8), for the total fifth-order process and the four possible cascade intermediates for the geometry of incoming beams shown in Fig. 2 with the angles listed in Table I.

Wave vector	F	$ F ^2$
Direct signal: $k_1 - k_2 - k_3 + k_4 + k_5$	0.7335 - 0.4703 <i>i</i>	0.759
Sequential intermediate: $k_1 - k_2 - k_3$	0.0024 - 0.0334 <i>i</i>	0.001
Sequential intermediate: $k_1 - k_2 + k_4$	0.0024 + 0.0334 <i>i</i>	0.001
Parallel intermediate: $k_1 - k_2 + k_5$	0.0002 - 0.0469 <i>i</i>	0.002
Parallel intermediate: $-k_3 + k_4 + k_5$	0.0022 - 0.0898 <i>i</i>	0.008

We define the integral over z as the phase matching factor, $F^{(n)}$. Figure 2(b) shows the calculated amplitude product of the five incoming fields, $a^{(n)}(z)$, integrated over the two dimensions orthogonal to z , for the employed beam geometry illustrated in Fig. 2(a). The z dependence of the spatial overlap between the incoming beams is well represented by a Gaussian distribution centered at $\frac{1}{2}$, shown as the solid line in Fig. 2(b). Using a Gaussian distribution to represent $a^{(n)}(z)$, the phase matching factor becomes

$$F^{(n)} = \int_0^l dz \exp[-b^2(z-d)^2] \exp(i \Delta k \cdot z), \quad (6)$$

with d equal to the displacement of the distribution along z ($d = \frac{1}{2}$) and b expressed in terms of the full width at half-maximum of the distribution, FWHM,

$$b^2 = \frac{4 \ln(2)}{(\text{FWHM})^2}. \quad (7)$$

The integral can be solved analytically to give the phase matching factor,

$$F^{(n)} = \frac{\sqrt{\pi}}{2b} \exp\left(\frac{i \Delta k l}{2} - \frac{\Delta k^2}{4b^2}\right) \left[\text{Erf}\left(\frac{bl}{2} + \frac{i \Delta k}{2b}\right) - \text{Erf}\left(\frac{bl}{2} + \frac{i \Delta k}{2b} - bl\right) \right]. \quad (8)$$

In the experiments presented here we have measured the intensity of the signal field, $|\varepsilon_s|^2$, and therefore the intensities of the signals are proportional to the modulus squared of the phase matching factors, $|F^{(n)}|^2$. Using Eq. (8) we have found an optimized geometry for the five incoming beams that minimizes $|F^{(3)}|^2$ for the four cascade intermediates while maximizing $|F^{(5)}|^2$ for the total fifth-order process. The values of $|F^{(n)}|^2$ are shown in Table II and the geometry for the incoming beams is shown in Fig. 2 with the angles for each beam in the sample listed in Table I. Note that the $|F^{(3)}|^2$ values only represent the degree of phase matching for the intermediate steps in the cascaded processes. The total cascaded processes requires additional consideration of the generated intermediate field along the length of the sample when calculating the phase matching factor for the second step in the cascade. While here we have not calculated the phase matching factor for the total cascaded processes, the product of the intermediate $|F^{(3)}|^2$ value and the direct $|F^{(5)}|^2$ value in Table II represents an upper limit for the magnitude of the phase matching factor for the total cascaded processes. The effect of the crossing distribution be-

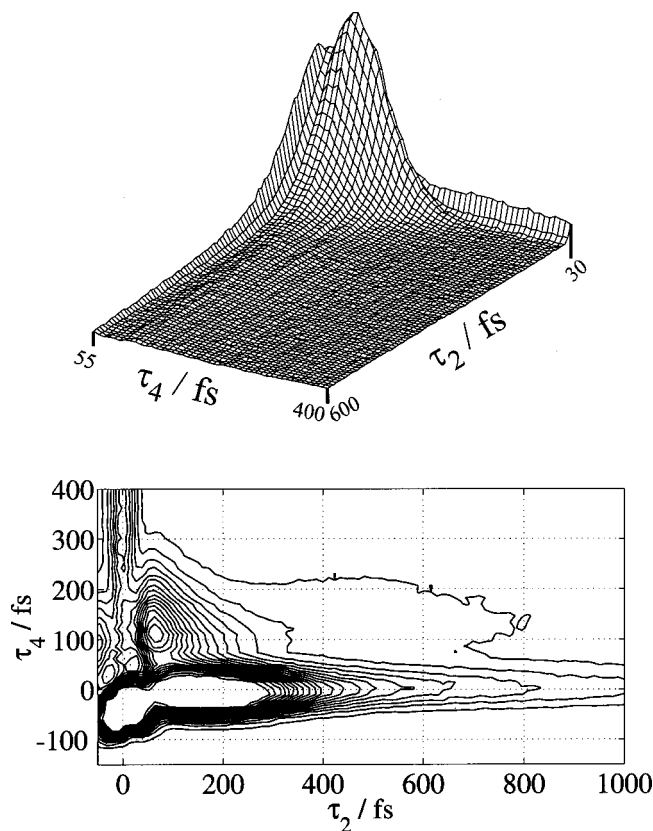


FIG. 3. The measured two-dimensional fifth-order response for CS₂ at room temperature with the polarizations of all of the incoming beams set parallel, $R_{zzzzz}^{(5)}$. The mesh plot is the three-dimensional representation of the contour plot with the ridges along $\tau_2=0$ and $\tau_4=0$ truncated: $\tau_2=30\text{--}600$ fs, $\tau_4=55\text{--}400$ fs.

tween the emitted intermediate cascade field and the remaining two incoming beams, along with the distance dependence of the intermediate field amplitude along the length of the sample, will serve to decrease the total phase matching factor for the cascaded processes. The total phase matching for the cascaded processes will be addressed in more detail in an upcoming manuscript.³¹

III. RESULTS

Figure 3 shows the two-dimensional time domain response for CS₂ at room temperature collected using the phase matching geometry shown in Fig. 2 with the polarization of all the incoming beams set parallel, $R_{zzzzz}^{(5)}$. The response is qualitatively different from the previously reported fifth-order signals for CS₂,^{5,8,11,12,14,16} which were attributed to the cascaded responses.²⁶ There is a large ridge along $\tau_4=0$ and a large response at the time origin where all five of the incoming pulses overlap in time, both of which are shown to go off scale in the contour plot displayed in Fig. 3. There is also a weak ridge along $\tau_2=0$ that decays very slowly. When one of the adjustable time variables is equal to zero, there may be contributions to the signal from one-dimensional fifth-order hyperpolarizability responses.¹³ In addition, along $\tau_2=0$ there can be contributions from the direct response that reflect population relaxation dynamics.^{32,33} In this manuscript we focus on the two-

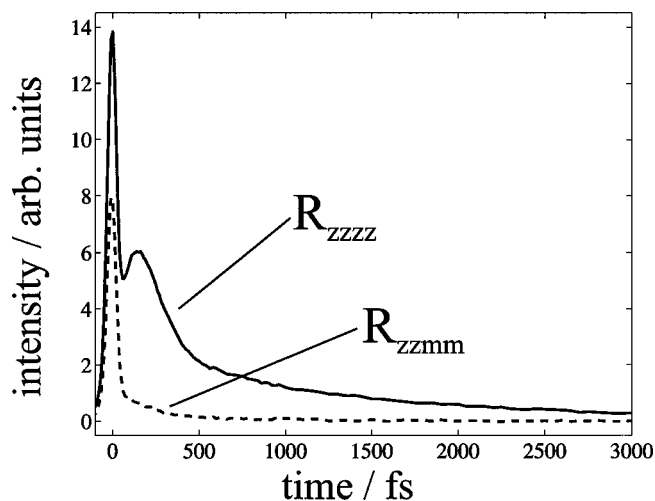


FIG. 4. Third-order nonresonant pump-probe measurement of CS₂ for two arrangements of the polarizations of the incoming beams: the solid line is $R_{zzzz}^{(3)}$, the dashed line is $R_{zzmm}^{(3)}$. Note that these are heterodyne measurements, and thus the response is linear in the signal field.

dimensional response, ($\tau_2>0, \tau_4>0$). We will address the response along the time axes in greater detail in a future manuscript.³¹

For a comparison of the two-dimensional spectra with both the cascaded and the third-order responses, the third-order responses were collected in a nonresonant pump-probe configuration and are shown in Fig. 4. The third-order measurements were in perfect agreement with previous third-order measurements for CS₂ at room temperature.^{34–36} The pump-probe signals are heterodyne detected, and thus the response is linear in the signal field. A one-dimensional slice from the two-dimensional response, along with the third-order response and the simulated parallel cascaded response, Eq. (1b), are shown in Fig. 5. For this comparison the third-order response has been squared to represent the homodyne detected signal, which is quadratic in the signal field. Note that when all of the polarizations of the incoming beams are parallel, $R_{zzzzz}^{(5)}$, the time dependence of the sequential cascaded responses along each of the two adjustable time variables will be the same as the third-order response, Eq. (1a). Based on the clear difference between the time-dependent response of the measured two-dimensional signal and direct simulations of the third-order cascades, in particular, the time dependence along τ_2 shown in Fig. 5, we exclude the cascaded responses and assign the major feature in the signal to the direct fifth-order response. The direct fifth-order response is peaked at ($\tau_2\sim 60$ fs, $\tau_4\sim 110$ fs) and rapidly decays within the first 400 fs along both of the adjustable time variables.

The dependence of the two-dimensional signal on the intensity of the incoming fields was measured and found to be fifth-order in the total intensity of the five incoming fields within the range of intensities used in these experiments (data not shown). While this measurement cannot be used to provide any discrimination between the cascaded and true fifth-order responses, since they both have the same dependence on the intensity of the incoming fields, it does demonstrate that our measured signal does not originate from a

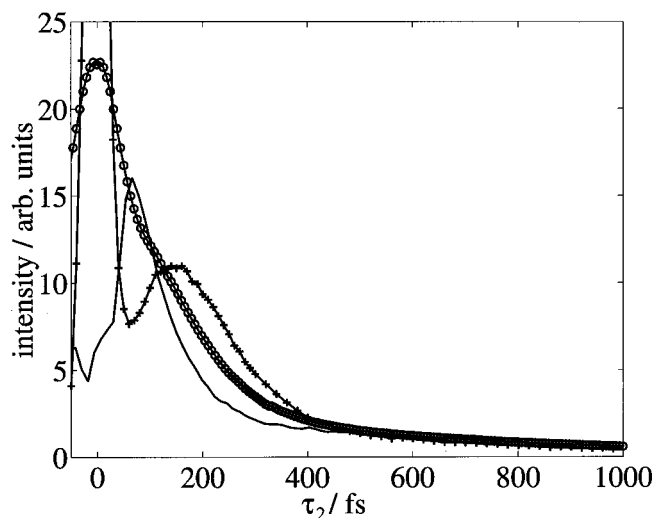


FIG. 5. A comparison of the one-dimensional slice from the two-dimensional response shown in Fig. 3 with the third-order response and the parallel cascaded response. The solid line is a slice along τ_2 for $\tau_4 = 120$ fs from the spectrum in Fig. 3. The line with the “+” markers is the third-order response. The line with the “o” markers is the simulated parallel cascaded response.

higher-order, for example seventh-order, process that could also be emitted along the same phase matched direction. It is important to exclude seventh-order signals since they do not require the same intrinsic nonlinearity in the response that is required by the fifth-order response. Therefore, they cannot be excluded simply by suggesting that the higher-order process should produce a much weaker signal.²⁹

In addition to the direct fifth-order response there is also a very weak response at longer times along τ_2 in Fig. 3 that is very asymmetric in its time-dependent response along the two adjustable time variables. The three-dimensional (3-D) mesh plot in Fig. 3 demonstrates how small this additional feature is compared with the dominant feature in the signal at earlier times. The asymmetry in the response of this additional feature, the signal decay is much slower along τ_2 than τ_4 , is similar to the time dependence of the parallel cascade response; see Ref. 26. For the reasons discussed in Ref. 26, such an asymmetric response is not consistent with the direct fifth-order response. Table II shows that, of the two types of cascaded responses, parallel and sequential, the parallel cascade intermediates are much better phase matched. Therefore, any underlying cascaded contribution to the signal should be dominated by the parallel cascade responses. The very small asymmetric contribution, which is most apparent in the two-dimensional contour plot in Fig. 3 at $\tau_2 > 400$ fs, could involve either the parallel cascaded signal alone or a cross-term between the direct fifth-order response and the parallel cascade response. It has been previously pointed out that, under perfect phase matching conditions, the signal field from the direct fifth-order response and the signal field from the cascaded responses will be phase shifted by 90° with respect to each other, thus eliminating any cross-term between the two signals.²⁹ However, the deviation from perfect phase matching, Table II, will produce phase rotation in the signals and allow for a nonzero cross-term.

A more detailed analysis of the signal field expressions,

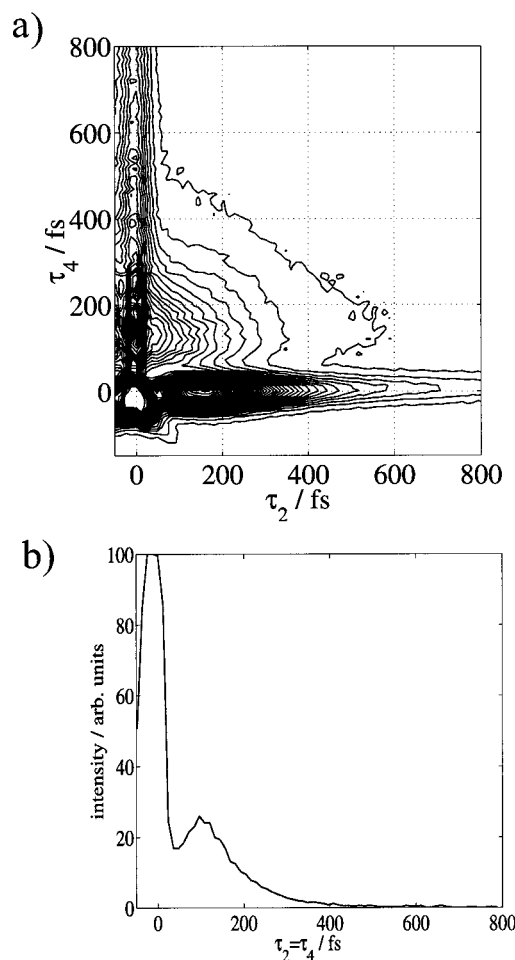


FIG. 6. (a) The measured two-dimensional fifth-order spectrum for CS_2 at room temperature with two of the polarizations of the incoming beams set at the magic angle, $m = 54.7^\circ$, $R_{zzzzmm}^{(5)}$. (b) A one-dimensional diagonal slice from the $R_{zzzzmm}^{(5)}$ spectrum.

including the total phase matching factors for the cascaded processes and a greater understanding of the proper definition for the number density of intermolecular chromophores, will be required to determine whether the small additional signal in the response in Fig. 3 is the result of a cross-term or the cascaded process alone. This work is currently underway in our laboratory and will be published in a subsequent article.³¹ In addition to identifying the origin of the small additional signal, the results should also provide quantitative information concerning the ratio for the magnitude of the third- to fifth-order response functions. Presently we will focus on the dominant feature in the signal, which we attribute to the direct fifth-order response.

Figure 6 shows the two-dimensional signal taken with the polarization of the first two interacting pulses rotated 54.7° (the magic angle, m) relative to the final three interacting pulses and the signal polarization, $R_{zzzzmm}^{(5)}$. The two-dimensional response is similar to that in Fig. 3 for $R_{zzzzzz}^{(5)}$, and peaked near the same position. The decay along each of the two time variables is slower than in the $R_{zzzzzz}^{(5)}$ signal; however, the time dependence is still qualitatively different than simulations of the cascaded responses for this set of polarizations of the incoming beams (not shown) from the

third-order measurements shown in Fig. 4. The fact that the measured time-dependent response is not consistent with the time dependence of the cascaded responses leads to the conclusion that the signal originates from the direct fifth-order response. In addition, the small asymmetric component that appears in the $R_{zzzzzz}^{(5)}$ signal is not found in the $R_{zzzzmm}^{(5)}$ signal. As explained in the discussion section, the $R_{zzzzmm}^{(5)}$ tensor element was chosen specifically to attempt to remove the small component related to the minor parallel cascaded contributions in the $R_{zzzzzz}^{(5)}$ signal.

IV. DISCUSSION

The origin of the electronically nonresonant fifth-order signal has been previously discussed in detail.^{1,2,4,13,18–20,24} The dynamical information is contained in the time domain response function, which for the two-dimensional signal can be expressed in terms of the polarizability operator as

$$R^{(5)}(\tau_2, \tau_4) = -\frac{1}{\hbar^2} \langle [[\hat{\alpha}(\tau_2 + \tau_4), \hat{\alpha}(\tau_2)], \hat{\alpha}(0)] \rho_{\text{eq}} \rangle. \quad (9)$$

The response functions can be expressed in terms of coordinates, Q_j , by Taylor expanding the polarizability operator,

$$\alpha(t) = \alpha_0 + \sum_j \alpha_j^{(1)} Q_j(t) + \frac{1}{2} \sum_{jk} \alpha_{j,k}^{(2)} Q_j(t) Q_k(t) + \dots, \quad (10)$$

where $\alpha^{(n)}$ is the n th derivative of the polarizability with respect to the coordinates. As mentioned in the Introduction, generation of the fifth-order signal requires nonlinearity in the form of either vibrational anharmonicity, AN, or nonlinearity in the polarizability, NP. In other words, if one makes the common assumption (Placzek approximation) that the polarizability is linear in the coordinates, truncating Eq. (10) at the first term, and one assumes the vibrational potential to be harmonic in the coordinates, Eq. (9) becomes zero. This demonstrates that the presence of at least one of these two sources of nonlinearity, AN or NP, between the basis nuclear motions, is necessary to generate a fifth-order signal. The response is then a sum of the two potential contributions:

$$R^{(5)}(\tau_2, \tau_4) = R^{(5),\text{AN}}(\tau_2, \tau_4) + R^{(5),\text{NP}}(\tau_2, \tau_4). \quad (11)$$

The anharmonic response is derived from inclusion of the cubic anharmonicity in the vibrational potential,

$$V \cong \frac{1}{2} \sum_j k_j Q_j^2 + \frac{1}{3!} \sum_{ijk} g_{ijk}^{(3)} Q_i Q_j Q_k. \quad (12)$$

In this expression $g_{ijk}^{(3)}$ is the magnitude of the cubic anharmonicity. The resulting fifth-order response function can be expressed in terms of two-point coordinate correlation functions,^{1,4,24} $G_j(t) \equiv -(i/2) \langle [Q_j(t), Q_j(0)] \rangle$,

$$R^{(5),\text{AN}}(\tau_2, \tau_4) \propto \sum_{ijk} g_{ijk}^{(3)} \alpha_i^{(1)} \alpha_j^{(1)} \alpha_k^{(1)} \times \int_0^\infty d\tau G_i(\tau_4 - \tau) G_j(\tau) G_k(\tau_2 - \tau). \quad (13)$$

The nonlinear polarizability response is generated by inclusion of the second term in the Taylor expansion of the polarizability, Eq. (10), and it can also be expressed in terms of two-point coordinate correlation functions, $G_j(t)$,

$$R^{(5),\text{NP}}(\tau_2, \tau_4) \propto \sum_{ij} [\alpha_{ij}^{(2)} \alpha_i^{(1)} \alpha_j^{(1)} G_i(\tau_4) G_j(\tau_2 + \tau_4) + \alpha_i^{(1)} \alpha_j^{(2)} \alpha_j^{(1)} G_i(\tau_4) G_j(\tau_2)]. \quad (14)$$

A comparison of these two expressions for the fifth-order response, Eqs. (13) and (14), with the expression for the third-order response, Eq. (15),

$$R^{(3)}(t) = \sum_j \alpha_j^{(1)} \alpha_j^{(1)} G_j(t), \quad (15)$$

makes it tempting to use the measured third-order response to determine a set of Raman active modes, $\alpha_j^{(1)} \alpha_j^{(1)} G_j(t)$, used to describe the intermolecular motions in the signal. This set of modes could then be used in Eqs. (13) and (14) to simulate the fifth-order response, leaving the cubic anharmonicity, $g_{ijk}^{(3)}$, and the nonlinearity in the polarizability, $\alpha_{ij}^{(2)}$, as adjustable parameters to be determined by fitting the measured fifth-order signal.

However, since the intermolecular spectrum is not resolved, fitting the third-order data requires the collection of the thousands of intermolecular nuclear modes into generalized time scales, for example, Brownian oscillators.³⁰ In order for the measured third-order response to be used as a basis for fitting the fifth-order response, an important assumption must be made concerning the generalized oscillators. In the case of anharmonicity, Eq. (13), one must assume that $g_{ijk}^{(3)}$ for all of the modes within each generalized oscillator are the same. For the case of nonlinear polarizability, Eq. (14), one must assume that $\alpha_{ij}^{(2)}$ is the same for all of the modes within each generalized oscillator. We find no *a priori* reason that either of these assumptions is reasonable. In fact, Murry *et al.* have used instantaneous normal mode calculations, INM, to demonstrate that in the case of the nonlinear polarizability model the assumption cannot be made for the intermolecular motions in CS₂.³⁷ The fact that the third-order response cannot be used as a basis for fitting the fifth-order data when measuring intermolecular motions was recently pointed out by Fourkas and co-workers, and this important point was not yet fully appreciated at the time of much of the previous work.^{22,37}

Since the fifth-order signals cannot be constructed from lower-order measurements, we will need to rely on simulations to help interpret the results. INM calculations by Fourkas and co-workers have found that the fifth-order response should, on average, be distributed into higher-frequency components of the intermolecular motions as compared with the third-order response.²² The comparison of our measured

third- and fifth-order responses in Fig. 5 shows that our measured fifth-order response is much faster than the third-order response, in good qualitative agreement with a larger relative weighting for higher-frequency motions, as predicted by the simulations.

Using INM and QNM (quenched normal mode) methods, Saito and Ohmine have generated the only simulations of the complete two-dimensional fifth-order response for CS₂.^{18,38} The simulations explicitly consider the nonlinear polarizability coupling, Eq. (14), and a comparison of the mesh plot of our data in Fig. 3 to the simulation in Fig. 7(b) of Ref. 18 demonstrates good agreement between the data and the simulation. Note the difference in convention for labeling of the time axes; we have labeled the two adjustable time variables τ_2 and τ_4 , while Saito and Ohmine have labeled the same two time variables t_1 and t_2 . Both responses peak at nearly the same location, and the time dependence along each of the two time variables is in good agreement.

One noticeable difference between our data and Fig. 7(b) of Ref. 18 is the small ridge that appears in the simulation along the time diagonal, $t_1 = t_2$. This ridge is an indication of the degree of inhomogeneity in the response on the time scale of the measurement.^{1,4,18} The rephasing capability of the system reflected along the diagonal of the two-dimensional response will be discussed further below. In Fig. 7(b) of Ref. 18 the only coupling mechanism considered was the coupling of modes through an interaction with the laser fields involving the second derivative of the polarizability, $\alpha_{ij}^{(2)} (i \neq j)$ in Eqs. (10) and (14), referred to as the “mode-mixing” term by Saito and Ohmine. When the authors added vibrational relaxation to the intermolecular modes in the form of the Brownian oscillator model, the diagonal ridge disappears from the simulation, Fig. 11(b) of Ref. 18. The resulting simulation is in excellent agreement with our measured data that does not contain evidence of a diagonal ridge. The Brownian oscillator model provides a model for vibrational relaxation via linear coupling of a given mode to the environment, which is modeled as a harmonic oscillator. However, the environment in this case is the very set of intermolecular motions under consideration. Thus, the introduction of vibrational relaxation by coupling to the environment is an introduction of coupling between the harmonic intermolecular modes. As a result, the physical basis of this coupling can be thought of as anharmonic coupling between the intermolecular modes. The agreement between Fig. 11(b) of Ref. 18 and our data, including the absence of the diagonal ridge in our data, provides direct evidence that the coupling between the intermolecular motions is not only mediated through the field-matter interaction, but there is also significant anharmonic coupling between the intermolecular motions in liquid CS₂.

We also note the small degree of participation in the fifth-order response from the longer time scale motions associated with diffusive reorientation. Even though these motions are not included in the INM/QNM calculations there is still excellent agreement between the simulations and the data. Diffusive reorientation is reflected in the third-order response for $t > 400$ fs, Fig. 4. A comparison of the third- and fifth-order responses demonstrates that the diffusive

components are almost completely absent from the fifth-order signal. The clear difference in the degree to which the diffusive reorientational motions participate in the third- and fifth-order responses again highlights the inability to use the third-order response as a basis for simulation of the fifth-order response. However, the relative success of our initial comparison between the data and the simulations suggests that a more detailed comparison of the experimental results with simulations will prove fruitful.

Figure 6 shows the two-dimensional signal for the tensor element with the polarizations of the first two interacting pulses rotated to the magic angle, 54.7° , $R_{zzzzmm}^{(5)}$. The response is similar to that of the $R_{zzzzzz}^{(5)}$ tensor; however, there are several notable differences. The small asymmetric component at long times along τ_2 in the $R_{zzzzzz}^{(5)}$ signal is not apparent in the $R_{zzzzmm}^{(5)}$ signal. As mentioned in the results section, we attribute this small feature to a signal that involves the parallel cascaded response, either the parallel cascaded signal alone or a cross-term between the direct fifth-order response and the parallel cascaded response. The absence of this feature in the $R_{zzzzmm}^{(5)}$ data demonstrates that the ratio of the direct fifth-order signal to the cascaded signals is larger for the case with the first two pulses set to the magic angle. The cascaded signals involve products of the third-order responses, Eq. (1), and the large decrease in the magnitude of the third-order response between $R_{zzzz}^{(3)}$ and $R_{zzmm}^{(3)}$, Fig. 4, means that the resulting parallel cascaded signals will be substantially reduced for $R_{zzzzmm}^{(5)}$. At early time the signal will be reduced by at least a factor of 10, and at later times the reduction will be even greater since the isotropic $R_{zzmm}^{(3)}$ response does not contain the longer time-scale responses associated with anisotropic diffusive motions.³⁹ On the other hand, INM calculations of Fourkas and co-workers suggest that the magnitude of the direct fifth-order response will not decrease significantly when going from $R_{zzzzzz}^{(5)}$ to $R_{zzzzmm}^{(5)}$.²² It should also be noted that while the $R_{zzmm}^{(3)}$ response only probes the isotropic motion and thus excludes diffusive motions, the $R_{zzzzmm}^{(5)}$ response does not isolate the isotropic motions, and, therefore, does not exclude the diffusive motions based on symmetry considerations alone.^{21,40} As a result, the $R_{zzzzmm}^{(5)}$ signal appears to be free of even the small level of contamination from the cascaded responses found in the $R_{zzzzzz}^{(5)}$ data.

Another difference between the $R_{zzzzmm}^{(5)}$ data and the $R_{zzzzzz}^{(5)}$ data, is that the relative intensity along the time diagonal, $\tau_2 = \tau_4$, is enhanced in the $R_{zzzzmm}^{(5)}$ data, and the response extends to longer times along $\tau_2 = \tau_4$. The time dependence along the time diagonal is an indication of the ability of the system to rephase.¹ A greater echolike contribution in the $R_{zzzzmm}^{(5)}$ signal compared with the $R_{zzzzzz}^{(5)}$ data might be an indication that the $R_{zzzzmm}^{(5)}$ tensor provides a greater weighting for Liouville pathways that can rephase. Both Fourkas and co-workers^{21,22} and Saito and Ohmine¹⁸ have discussed the fact that the $R_{zzzzzz}^{(5)}$ tensor will weight all Liouville pathways equally and, as a result, should not strongly reflect the rephasing ability of the system. The reader is directed to Refs. 18, 21 and 22 for more detailed discussions.

The time dependence along the time diagonal for $R_{zzzzmm}^{(5)}$ is shown in Fig. 6. The signal decays rapidly beyond 100 fs and is almost completely gone by 400 fs. Therefore, even though the $R_{zzzzmm}^{(5)}$ response retains the rephasing ability for a longer time than the $R_{zzzzzz}^{(5)}$ response, the rephasing ability is still lost very rapidly. The measurement demonstrates that the intermolecular motions maintain a coherent memory of their frequency for less than 400 fs. Since this time scale is directly comparable to, or faster than, the time scales associated with the intermolecular motions, 0–200 cm^{-1} , this measurement is a direct indication that the intermolecular spectrum of liquid CS_2 at room temperature is essentially homogeneous. As discussed above, the comparison between the simulated $R_{zzzzzz}^{(5)}$ response and our measured $R_{zzzzzz}^{(5)}$ data indicated that the coupling between the intermolecular motions that is responsible for the rapid loss of rephasing ability is an intrinsic, or anharmonic, coupling that does not involve the coupling induced by the light matter interactions. The conclusion that the intermolecular spectrum is well described as homogeneous is in contrast to the conclusions inferred from third-order measurements on binary mixtures of CS_2 and alkane solvents.³⁵

V. CONCLUSION

In our previous work we demonstrated that all previous measurements of the electronically nonresonant fifth-order response for the intermolecular motions in liquid CS_2 were dominated by third-order cascaded responses.²⁶ Here we have shown that phase matching can be used to provide significant discrimination against the cascaded responses, allowing the direct fifth-order signal to be measured. We have also demonstrated that the tensoral nature of the response can be used to provide additional discrimination against the cascaded contributions. We are currently investigating the tensoral nature of the response in depth, and this work will appear in a forthcoming manuscript.³¹ From our data we conclude that the intermolecular spectrum of CS_2 at room temperature is well described as homogeneous. Our data show good agreement with INM/QNM simulations. The agreement between the data and simulations is promising, and it cannot be over emphasized that simulation work and theoretical modeling will be essential to the success of the technique since measured lower- (third-) order data cannot be used as a basis for the interpretation of the fifth-order data. We hope measurements reported here will provide incentive for improved simulations and modeling and stimulate further improvement of the experimental technique, so that the promise of 2D spectroscopy for the study of liquid dynamics is realized.

ACKNOWLEDGMENT

This research was supported by a grant from NSF (Grant No. CHE-9319692).

- ¹Y. Tanimura and S. Mukamel, *J. Chem. Phys.* **99**, 9496 (1993).
- ²S. Mukamel, A. Piryatinski, and V. Chernyak, *Acc. Chem. Res.* **32**, 145 (1999).
- ³S. Mukamel, A. Piryatinski, and V. Chernyak, *J. Chem. Phys.* **110**, 1711 (1999).
- ⁴V. Chernyak and S. Mukamel, *J. Chem. Phys.* **108**, 5812 (1998).
- ⁵K. Tominaga and K. Yoshihara, *J. Chem. Phys.* **104**, 4419 (1996).
- ⁶K. Tominaga and K. Yoshihara, *J. Chem. Phys.* **104**, 1159 (1996).
- ⁷K. Tominaga and K. Yoshihara, *Phys. Rev. Lett.* **74**, 3061 (1995).
- ⁸K. Tominaga, G. P. Keogh, Y. Naitoh, and K. Yoshihara, *J. Raman Spectrosc.* **26**, 495 (1995).
- ⁹A. Tokmakoff, M. J. Lang, D. S. Larsen, G. R. Fleming, V. Chernyak, and S. Mukamel, *Phys. Rev. Lett.* **79**, 2702 (1997).
- ¹⁰A. Tokmakoff, M. J. Lang, D. S. Larsen, and G. R. Fleming, *Chem. Phys. Lett.* **272**, 48 (1997).
- ¹¹A. Tokmakoff and G. R. Fleming, *J. Chem. Phys.* **106**, 2569 (1997).
- ¹²A. Tokmakoff, M. J. Lang, X. J. Jordanides, and G. R. Fleming, *Chem. Phys.* **233**, 231 (1998).
- ¹³T. Steffen, J. T. Fourkas, and K. Duppen, *J. Chem. Phys.* **105**, 7364 (1996).
- ¹⁴T. Steffen and K. Duppen, *Phys. Rev. Lett.* **76**, 1224 (1996).
- ¹⁵T. Steffen and K. Duppen, *Chem. Phys. Lett.* **273**, 47 (1997).
- ¹⁶T. Steffen and K. Duppen, *J. Chem. Phys.* **106**, 3854 (1997).
- ¹⁷T. Steffen and K. Duppen, *Chem. Phys. Lett.* **290**, 229 (1998).
- ¹⁸S. Saito and I. Ohmine, *J. Chem. Phys.* **108**, 240 (1998).
- ¹⁹K. Okumura and Y. Tanimura, *J. Chem. Phys.* **107**, 2267 (1997).
- ²⁰K. Okumura and Y. Tanimura, *J. Chem. Phys.* **106**, 1687 (1997).
- ²¹R. L. Murry and J. T. Fourkas, *J. Chem. Phys.* **107**, 9726 (1997).
- ²²R. L. Murry, J. T. Fourkas, and T. Keyes, *J. Chem. Phys.* **109**, 7913 (1998).
- ²³S. Mukamel, A. Piryatinski, and V. Chernyak, *Acc. Chem. Res.* **32**, 145 (1999).
- ²⁴M. Cho, in *Advances in Multi-Photon Processes and Spectroscopy*, edited by S. H. Lin, A. A. Villaeys, and Y. Fujimura (World Scientific, Singapore, 1999), Vol. 12, pp. 229.
- ²⁵D. J. Ulness, J. C. Kirkwood, and A. C. Albrecht, *J. Chem. Phys.* **108**, 3897 (1998).
- ²⁶D. Blank, L. Kaufman, and G. R. Fleming, *J. Chem. Phys.* **111**, 3105 (1999).
- ²⁷J. D. Hybl, A. W. Albrecht, S. M. Gallagher Faeder, and D. M. Jonas, *Chem. Phys. Lett.* **297**, 307 (1998).
- ²⁸T. Joo, Y. W. Jia, and G. R. Fleming, *Opt. Lett.* **20**, 389 (1995).
- ²⁹M. Cho, D. A. Blank, J. Sung, K. Park, S. Hahn, and G. R. Fleming, *J. Chem. Phys.* **112**, 2082 (2000).
- ³⁰S. Mukamel, *Principles of Nonlinear Optical Spectroscopy*, 1st ed. (Oxford University Press, New York, 1995).
- ³¹L. J. Kaufman, D. A. Blank, and G. R. Fleming (unpublished).
- ³²T. Steffen and K. Duppen, *Chem. Phys.* **233**, 267 (1998).
- ³³V. Chernyak, A. Piryatinski, and S. Mukamel, *Laser Chem.* **19**, 109 (1999).
- ³⁴S. Ruhman, A. G. Joly, and K. A. Nelson, *IEEE J. Quantum Electron.* **24**, 460 (1988).
- ³⁵D. McMorro, N. Thantu, J. S. Melinger, S. K. Kim, and W. T. Lotshaw, *J. Phys. Chem.* **100**, 10 389 (1996).
- ³⁶W. T. Lotshaw, D. McMorro, N. Thantu, J. S. Melinger, and R. Kitchenhams, *J. Raman Spectrosc.* **26**, 571 (1995).
- ³⁷R. L. Murry, J. T. Fourkas, and T. Keyes, *J. Chem. Phys.* **109**, 2814 (1998).
- ³⁸After submission of this paper we became aware of new simulations on atomic liquids that appear to show very similar two-dimensional responses compared with our measured responses reported in this paper; A. Ma and R. M. Strat (unpublished).
- ³⁹B. J. Berne and R. Pecora, *Dynamic Light Scattering* (Kreiger, Malabar, FL, 1990).
- ⁴⁰A. Tokmakoff, *J. Chem. Phys.* **105**, 13 (1996).